
# FLEXURAL BEHAVIOR OF CONCRETE BEAMS PRESTRESSED WITH HYBRID TENDONS

Adi A. Obeidah, Ph.D.
HNTB Cooperation
Project Engineer

Hani Nassif, P.E., Ph.D., FACI
Rutgers Infrastructure Monitoring and Evaluation (RIME) Group
Professor and Director

THE WORLD'S GATHERING PLACE FOR ADVANCING CONCRETE

aci CONCRETE CONVENTION

- Introduction
- Experimental Program
- ACI Design Guide Provisions
- Finite Element Modeling
- Conclusions

# Background and Motivation

- Hybrid prestressed systems are defined as combined bonded steel tendons with unbonded CFRP or steel tendons relatively a new class of prestressed concrete members requiring further research.
- Used in segmental bridges and retrofitting and rehabilitation of existing damaged members.
- Testing results exhibited good control of cracking and enhanced carrying-capacity, without significant reduction of the system ductility or deformability.

# Background and Motivation

- Unbonded steel strands are vulnerable to chloride attacks raising the risk of the strands' brittle failure.
- Corrosion promoted by chloride attacks or inadequate grouting, does not always generate visible warning signs (cracks or corrosion stains) making it difficult to detect during inspections.

Menga et al. (2023) "Corrosion-induced damages and failures of posttensioned bridges: A literature review." *Structural Concrete* 24.1 84-99.

# Background and Motivation

- A recent study analyzing the corrosion-induced failure of segmental and box-beam bridges post-tensioned with grouted steel tendons revealed that no warning signs were visible prior to tendon failure (system failure/collapse) for most of those bridges resulting in personal injury and substantial loss of life, property, and loss of infrastructure, especially that some of these bridges were just 9 years old

Menga et al.(2023) "Corrosion-induced damages and failures of posttensioned bridges: A literature review." *Structural Concrete* 24.1 84-99.

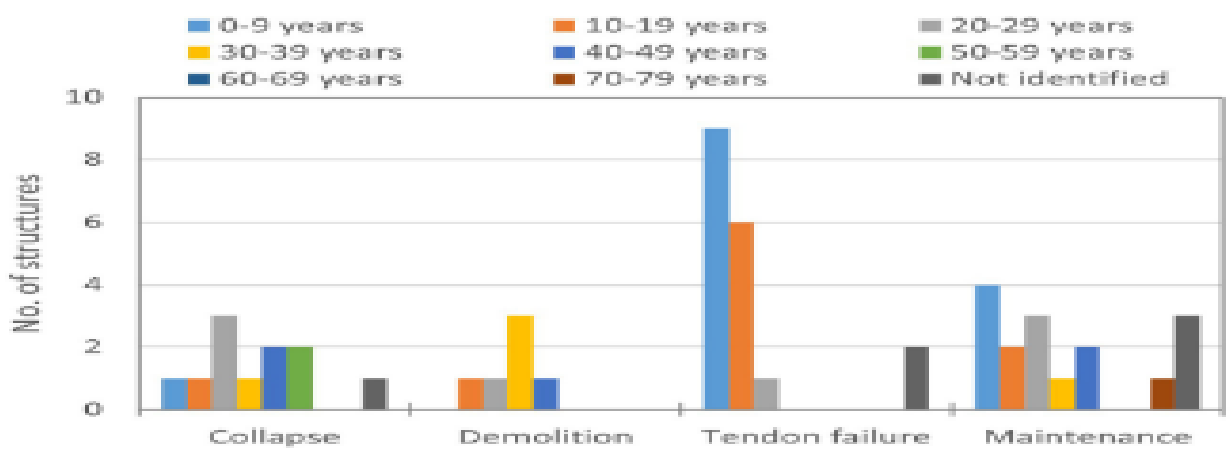

# Background and Motivation

- Due to its inherent corrosion resistance, the advantages of incorporating FRP tendons in prestressed girder systems are tremendous. FRP tendons have a superior strength-to-weight ratio and excellent fatigue resistance.
- The linear-elastic nature of FRP tendons exhibit brittle flexural failure when exclusively used in prestressed members, which restricts their implementation in prestressed concrete bridges.
- Driven by the need of innovative sustainable designs, incorporating multiple tendon materials (steel and CFRP) in a hybrid prestressed system offers a unique synergy that would improve durability at no-cost to the system ductility.

## Objective(s)

- Assess the impact of combining unbonded CFRP tendons with bonded steel tendons on the overall flexural structural behavior at serviceability and ultimate limit states based on:
  - ✓ laboratory testing of eighteen hybrid prestressed beams.
  - ✓ analytical evaluation following current practice and using finite element modeling.

# **Experimental Program:** Beam Testing Set-up & Dimensions (cm)

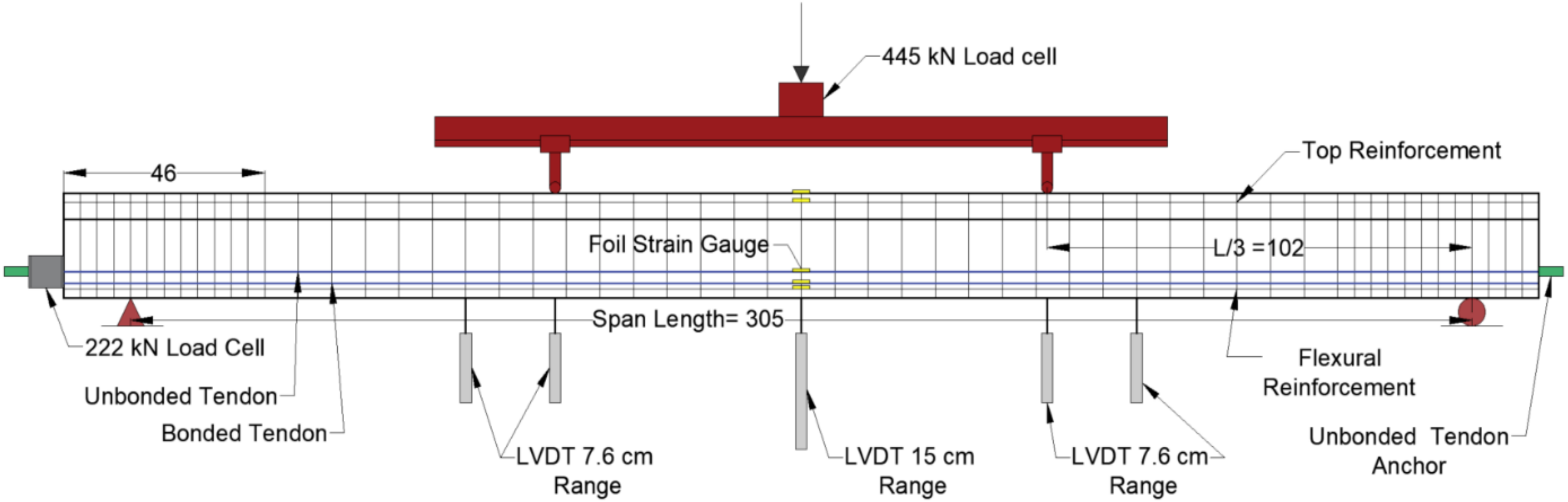


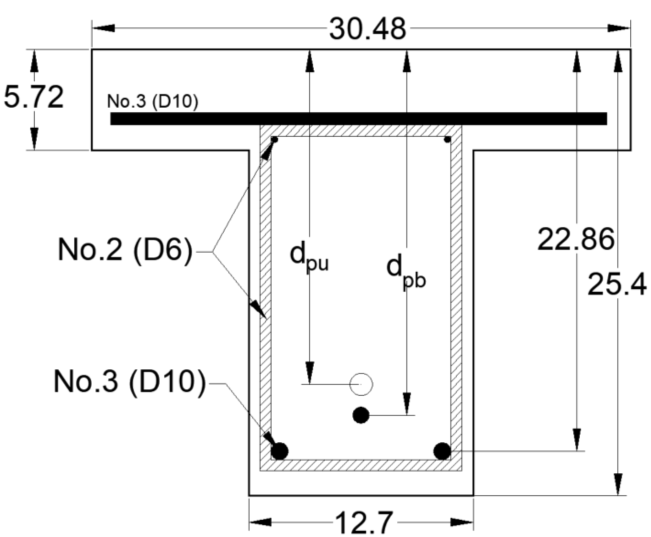


*Hybrid Beams*

Notation: Hx-AD[1]-AD[2], H: Hybrid beam, x: Unbonded Tendon Material – F = CFRP and S = Steel, A: Prestressing System – U for Unbonded and B for Bonded, D: 2 for strand diameter (φ) 5/16”, 3 for φ3/8”, and 4 for φ½” tendons,

aci CONCRETE CONVENTION

# Experimental Program (cont'd)

| Beam Group | Beam No. | Designation | Bonded Tendon | | | Unbonded Tendon | | | $L/d_e$ | $\omega_e$ | L (m) |
|---|---|---|---|---|---|---|---|---|---|---|---|
| | | | $f_{pe(B)}$ (MPa) | $A_{psB}$ ($mm^2$) | $d_{pB}$ (cm) | $f_{pe(U)}$ (MPa) | $A_{psU}$ ($mm^2$) | $d_{pU}$ (cm) | | | |
| Control | 1 | BS-2-3 | 1282 | 55 | 22 | 1145 | 55 | 19 | 14.3 | 0.055 | 3 |
| | 2 | BS-2-2 | 1284 | 37.4 | 22 | 1326 | 37.4 | 16.9 | 14.3 | 0.037 | 3 |
| Unbonded Steel | 3 | US-2-3 | - | - | - | 1055 | 55 | 19 | 16.8 | 0.050 | 3 |
| | | | - | - | - | 1020 | 55 | 22 | | | |
| | 4 | US-1-3 | - | - | - | 1103 | 55 | 15.6 | 17.6 | 0.039 | 3 |
| | 5 | US-1-4 | - | - | - | 1027 | 99 | 15.6 | 13.9 | 0.049 | 3 |
| Unbonded CFRP | 6 | UF-1-3* | - | - | - | 1165 | 71 | 15.6 | 17.4 | 0.049 | 2.4 |
| | 7 | UF-1-3 | - | - | - | 1276 | 71 | 15.6 | 18.0 | 0.050 | 3 |
| | 8 | UF-1-4 | - | - | - | 1027 | 123 | 15.6 | 16.8 | 0.064 | 3 |
| Hybrid Steel | 9 | HS-U3-B3 | 1082 | 55 | 22 | 1089 | 55 | 19 | 14.3 | 0.048 | 3 |
| | 10 | HS-B3-U3 | 1213 | 55 | 22 | 1289 | 55 | 15.6 | 15.3 | 0.048 | 3 |
| | 11 | HS-B3-U4 | 1179 | 55 | 22 | 965 | 99 | 15.6 | 16.1 | 0.077 | 3 |
| | 12 | HS-B4-U4 | 1117 | 99 | 22 | 1082 | 99 | 15.6 | 15.6 | 0.104 | 3 |
| Hybrid Steel-CFRP | 13 | HF-B2-U3 | 1052 | 37.4 | 22 | 1230 | 71 | 16.9 | 15.6 | 0.055 | 3 |
| | 14 | HF-B2-U3d^ | 1033 | 37.4 | 22 | 1380 | 71 | 19 | 15.6 | 0.052 | 3 |
| | 15 | HF-U3-B3 | 1469 | 55 | 22 | 1165 | 71 | 19 | 14.2 | 0.060 | 3 |
| | 16 | HF-B3-U3 | 1220 | 55 | 22 | 1551 | 71 | 15.6 | 15.9 | 0.071 | 3 |
| | 17 | HF-B3-U4 | 1200 | 55 | 22 | 1082 | 123 | 15.6 | 16.7 | 0.102 | 3 |
| | 18 | HF-B4-U3 | 1110 | 99 | 22 | 1503 | 71 | 15.6 | 15.4 | 0.077 | 3 |

$$\omega_e = \frac{A_{psB} f_{puB} + A_{psU} f_{puU} + A_s f_y - A'_s f'_y}{b d_e f'_c} \qquad d_e = \frac{A_{psB} f_{puB} d_{pB} + A_{psU} f_{puU} d_{pU} + A_s f_y d_s}{A_{psB} f_{puB} + A_{psU} f_{puU} + A_s f_y}$$

The effective reinforcing index ($\omega_e$) and the effective flexural reinforcement depth ($d_e$) defined by Naaman (1994) are modified slightly by the authors to utilize $f_{pu}$ instead of $f_{ps}$,

# Experimental Program – Load versus Mid-Span Deflection

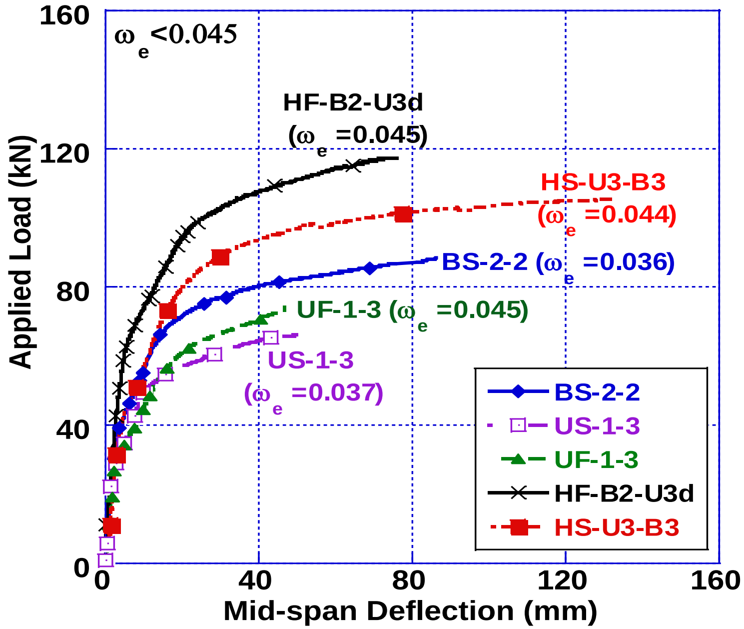


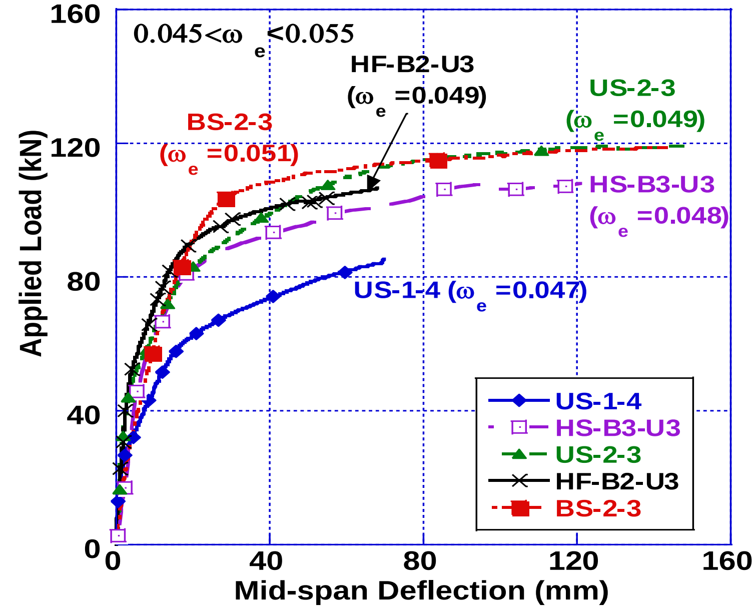


- For beam with similar ($\omega_e$), replacing bonded tendons with unbonded tendons resulted in a reduction in the load and deflections at the cracking and ultimate stages.
- Beams US-1-4 ($\omega_{e(s)}$=0.047) and UF-1-3 ($\omega_{e(s)}$=0.045) achieved a lower cracking load by 48 and 39% and deflections by 62 and 45%, compared to the bonded beam BS-2-3 ($\omega_{e(s)}$=0.051), respectively.
- The failure load decreased by 33% for both beams (US-1-4, UF-1-3), compared to the bonded beam BS-2-3

# Experimental Program – Load versus Mid-Span Deflection

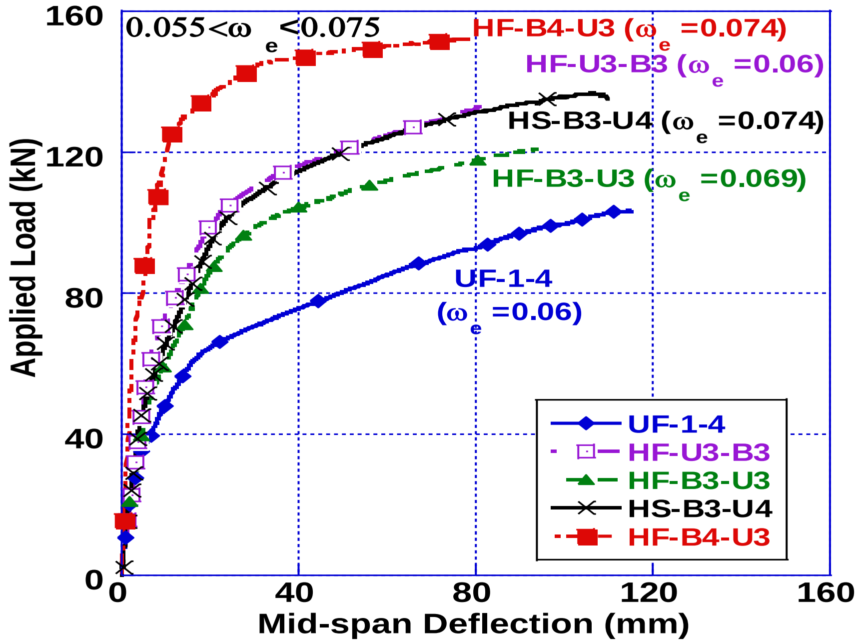


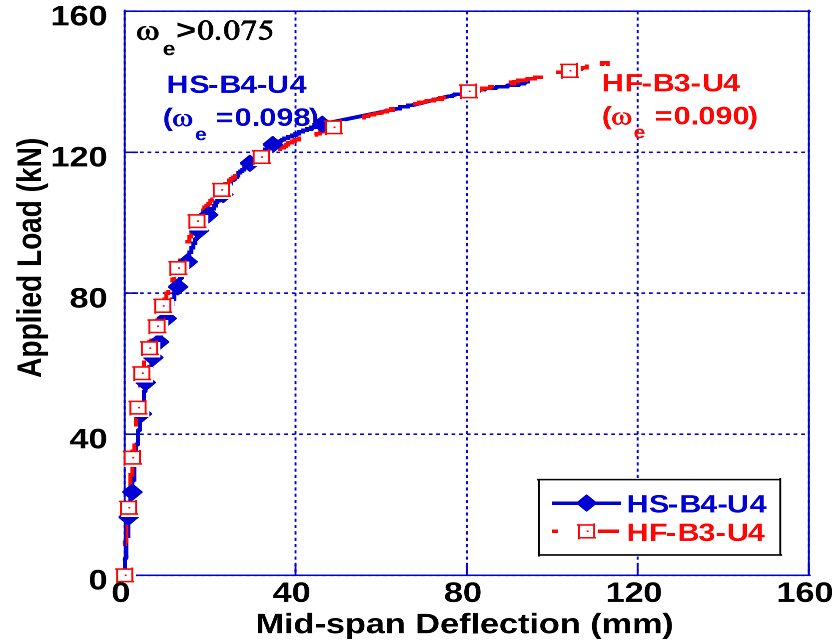


- Testing results show that hybrid steel-CFRP beams (HF-B3-U4 with $\omega_e$=0.09 and HF-B4-U3 with $\omega_e$=0.074) achieved strength limit state loads of 147, and 151 kN at 117 and 79 mm of deflection
- Compared to hybrid-steel beam HS-B4-U4 ($\omega_e$=0.098), hybrid-CFRP beam HF-B3-U4 ($\omega_e$=0.09) achieved similar ultimate moment capacity at failure with an ultimate deflection increase of +18%. On the other hand, a reduction of 28% in deflection was observed in HF-B4-U3 ($\omega_e$=0.074) compared to HS-B3-U3 ($\omega_e$=0.074).

# Experimental Program – Ductility Indices

| Designation | $\omega_e$ | $M_{cr}$ | $\Delta_{cr}$ | $M_y$ | $\Delta_y$ | $M_u$ | $\Delta_u$ | $\mu_y$ | $\mu_{zou}$ | $\varepsilon_t$^ |
|---|---|---|---|---|---|---|---|---|---|---|
| **US-1-4** | 0.047 | 1400 | 3.6 | 2850 | 25 | 4000 | 51 | 20 | 40 | 0.006 |
| **UF-1-3** | 0.045 | 1650 | 2.5 | 2050 | 16 | 4000 | 58 | 4 | 56 | 0.004 |
| **%** | **-4.3** | **18** | **-31** | **-28** | **-36** | **0** | **14** | **-80** | **40** | **-33** |
| **UF-1-4** | 0.06 | 1700 | 4.3 | 2600 | 12 | 5100 | 140 | 12 | 98 | 0.009 |
| **HF-U3-B3** | 0.06 | 3100 | 6.6 | 4550 | 17 | 6650 | 81 | 5 | 26 | 0.015 |
| **%** | **0.0** | **82** | **54** | **75** | **42** | **30** | **-42** | **-58** | **-74** | **67** |
| **HS-U3-B3** | 0.044 | 2250 | 5 | 3150 | 11 | 5550 | 132 | 12 | 61 | 0.015 |
| **HF-B2-U3d*** | 0.045 | 2600 | 4 | 4400 | 17 | 5850 | 76 | 4 | 45 | 0.01 |
| **%** | **2.3** | **16** | **-20** | **40** | **55** | **5** | **-42** | **-67** | **-26** | **-33** |
| **HS-B3-U3** | 0.048 | 2650 | 8 | 3350 | 12 | 5350 | 122 | 10 | 31 | 0.019 |
| **HF-B2-U3*** | 0.049 | 2250 | 3 | 4250 | 16 | 5300 | 68 | 4 | 53 | 0.008 |
| **%** | **2.1** | **-15** | **-63** | **27** | **33** | **-0.9** | **-44** | **-60** | **71** | **-58** |
| **HS-B3-U4** | 0.074 | 2350 | 5 | 4750 | 16 | 6900 | 109 | 7 | 67 | 0.008 |
| **HF-B3-U3** | 0.069 | 2700 | 4 | 4100 | 23 | 6000 | 99 | 4 | 54 | 0.018 |
| **%** | **-6.8** | **15** | **-20** | **-14** | **44** | **-13** | **-9** | **-43** | **-19** | **125** |
| **HS-B3-U4** | 0.074 | 2350 | 5 | 4750 | 16 | 6900 | 109 | 7 | 67 | 0.008 |
| **HF-B4-U3** | 0.074 | 3500 | 3 | 6100 | 5 | 7550 | 79 | 15 | 57 | 0.009 |
| **%** | **0.0** | **49** | **-40** | **28** | **-69** | **9** | **-28** | **114** | **-15** | **13** |
| **HS-B4-U4** | 0.098 | 2900 | 6 | 5000 | 19 | 7350 | 99 | 5 | 43 | 0.007 |
| **HF-B3-U4** | 0.09 | 2950 | 5 | 5100 | 18 | 7350 | 117 | 7 | 57 | 0.015 |
| **%** | **-8.2** | **1.7** | **-17** | **2** | **-5** | **0.0** | **18** | **40** | **33** | **114** |

*** $\varepsilon_{cu}$ = 0.019 ~ 0.022, 1 kN = 0.225 kip, 1 inch = 25.4 mm**
**^Net tensile strain at the non-prestressed reinforcements excluding strains induced due to creep, prestressing, or shrinkage**

$$\mu_{Zou} = \frac{M_u}{M_{cr}} \cdot \frac{\Delta_u}{\Delta_{cr}}$$

$$\mu_{\Delta} = \frac{\Delta_u}{\Delta_y}$$

***Ductility Results***

- Three ductility indices are utilized, which are the conventional deformation index ($\mu_y = \Delta_u/\Delta_y$), Zou (2003) expression, and the net tensile strain method defined in ACI 318.
- Compared to the other two methods, the net tensile strain method adopted in ACI318 shows a reasonable trend with the effective reinforcement ratio for unbonded and hybrid CFRP-steel beams.
- CFRP hybrid beams shows an increase in the net tensile strain (Δεt) for CFRP prestressed beam with $\omega_{e(s)}$ equal or exceeding 0.06, ranging between 13 to 125%. On the other hand, a decrease in the net tensile strain (Δεt) ranging between 33 to 58% is observed with CFRP prestressed beams with $\omega_{e(s)}$ less than 0.06.

FRPRCS 16

RUTGERS Infrastructure Monitoring and Evaluation (RIME)

# Experimental Program – Flexural Member Failure Criteria

- According to ACI 440.4R, a ***compression-controlled (CC)*** *section occurs when the concrete crushes ($\varepsilon_{cu}$=~0.003) before the failure of the tendons, while a* ***tension-controlled (TC) section*** *takes place when the failure of the member is governed by the tensile capacity of the tendon ($\varepsilon_{cu}$<<0.003)*. ACI 440.4R identifies those section during the design phase based on the concept of the balanced ratio ($\rho_b$) in which TC sections can be achieved with prestressed reinforcement ratio less than the balanced ratio ($\rho_b$), while CC sections required a prestressed reinforcement ratio larger than $\rho_b$.
- Unlike ACI 440.4R, ACI 318 relies on the net tensile strain in the outermost tension reinforcement in the critical section. TC ***sections*** *are defined as members in which the net tensile strain $\varepsilon_t$ at the level of the outermost tension reinforcement developed when the outermost concrete compressive strain $\varepsilon_{cu}$ reaches 0.003 is greater than or equal to 0.005 ($\varepsilon_t \geq 0.005$) for prestressed reinforcement and $\varepsilon_{ty}$ + 0.003 ($\varepsilon_t \geq \varepsilon_{ty} + 0.003$) for non-prestressed reinforcements.*

aci CONCRETE CONVENTION

# Experimental Program – Flexural Member Failure Criteria

| Beam | $d_{e(s)}$ | $\omega_{e(s)}$ | reinforcement ratio, % | | | $\varepsilon_{cu}$ | ACI 318-19^ | | ACI 440.4R** | |
|---|---|---|---|---|---|---|---|---|---|---|
| | | | $\rho_{pB}$ | $\rho_{pU}$ | $\rho_{tot}$ | | $\varepsilon_t$^^ | Flexural behavior | RF* | Flexural behavior |
| BS-2-3 | 212.3 | 0.051 | 0.18 | - | 0.38 | 0.0031 | 0.019 | TC | x | CC |
| BS-2-2 | 205.7 | 0.036 | 0.13 | - | 0.33 | 0.0022 | 0.026 | TC | ✓ | TC |
| US-2-3 | 212.3 | 0.049 | - | 0.18 | 0.38 | 0.0029 | 0.023 | TC | x | CC |
| US-1-3 | 181.6 | 0.037 | - | 0.12 | 0.32 | 0.0026 | 0.077 | TC | x | CC |
| US-1-4 | 173.0 | 0.047 | - | 0.21 | 0.41 | 0.0027 | 0.006 | TC | x | CC |
| UF-1-3* | 175.3 | 0.042 | - | 0.15 | 0.35 | 0.0026 | 0.004 | TR | x | CC |
| UF-1-3 | 175.3 | 0.045 | - | 0.15 | 0.35 | 0.0028 | 0.009 | TR | x | CC |
| UF-1-4 | 168.9 | 0.060 | - | 0.26 | 0.46 | 0.0027 | 0.015 | TC | x | CC |
| HS-U3-B3 | 212.3 | 0.044 | 0.09 | 0.08 | 0.38 | 0.0030 | 0.0194 | TC | x | CC |
| HS-B3-U3 | 198.6 | 0.048 | 0.08 | 0.12 | 0.40 | 0.0029 | 0.0084 | TC | x | CC |
| HS-B3-U4 | 189.0 | 0.074 | 0.08 | 0.21 | 0.49 | 0.0028 | 0.0072 | TC | x | CC |
| HS-B4-U4 | 195.6 | 0.098 | 0.15 | 0.21 | 0.56 | 0.0029 | 0.0075 | TC | x | CC |
| HF-B2-U3 | 195.6 | 0.049 | 0.06 | 0.14 | 0.40 | 0.0022 | 0.0103 | TC | ✓ | TC |
| HF-B2-U3d | 195.6 | 0.045 | 0.06 | 0.14 | 0.40 | 0.0019 | 0.0150 | TC | ✓ | TC |
| HF-U3-B3 | 214.6 | 0.060 | 0.09 | 0.10 | 0.40 | 0.0029 | 0.0180 | TC | ✓ | CC |
| HF-B3-U3 | 191.8 | 0.069 | 0.08 | 0.15 | 0.43 | 0.0029 | 0.0088 | TC | ✓ | CC |
| HF-B3-U4 | 183.1 | 0.090 | 0.08 | 0.26 | 0.54 | 0.0030 | 0.0150 | TC | x | CC |
| HF-B4-U3 | 198.4 | 0.074 | 0.15 | 0.15 | 0.50 | 0.0031 | 0.0259 | TC | ✓ | CC |

- These results shows that hybrid CFRP-Steel beams can achieve the same failure modes observed in hybrid steel beams without sacrificing any portion of the capacity and deformability of the section.
- Hybrid CFRP-steel beams could achieve as much net tensile-strain and more, compared to hybrid-steel beams with similar $\omega_e$ ratios.
- HF-B2-U3 and HS-B3-U3 ($\omega_e$=0.049, $\omega_e$=0.048) achieved a net tensile strain of 0.0103 and 0.0084, respectively, which designates both as tension-controlled members in accordance with ACI 318, even though one of them failed in concrete crushing, while the other failed by the rupture of the non-prestressed reinforcement.

# ACI Design Guide Provisions: <u>*ACI 440.4R-04*</u>

$$I_e = \left(\frac{M_{cr}}{M_a}\right)^3 \beta_d I_g + \left[1 - \left(\frac{M_{cr}}{M_a}\right)^3\right] I_{cr} \le I_g \qquad \beta_d = 0.5\left[\frac{E_p}{E_s} + 1\right]$$

$$I_{cr} = \frac{b(c_{cr})^3}{3} + nA_{psB}(d_{psB} - c_{cr})^2 + nA_{psU}(d_{psU} - c_{cr})^2 + nA_s(d_s - c_{cr})^2$$

$$f_{psB} = f_{peB} + E_{psB}\varepsilon_c\left(\frac{d_{pB}}{c} - 1\right)$$

$$f_{psU} = f_{peU} + \Omega E_{psU}\varepsilon_c\left(\frac{d_{pU}}{c} - 1\right) \quad \text{where} \quad \Omega = \frac{5.4}{L/d_p}$$

$$A_{psB}f_{psB} + A_{psU}f_{psU} + A_s f_y - A'_s\left|f'_y\right| = 0.85\beta_1 f'_c(b - b_w)h_f + 0.85\beta_1 f'_c b_w c_{cr}$$

$$M_n = A_{psB}f_{psB}\left(d_{pB} - \frac{a}{2}\right) + A_{psU}f_{psU}\left(d_{pU} - \frac{a}{2}\right) + A_s f_y\left(d_s - \frac{a}{2}\right) - A'_s\left|f'_y\right|\left(d'_s - \frac{a}{2}\right) + 0.85\beta_1 f'_c(b - b_w)h_f\left(\frac{a - h_f}{2}\right)$$

**<u>Note:</u>** For tested beams with hybrid tendons, AASHTO uses $A_{psB}f_{psB} + A_{psU}f_{pse}$ (instead of $A_{psB}f_{psB} + A_{psU}f_{psU}$) to satisfy the equilibrium of forces and the weighted average stress ($f_{ps(WA)}$) in the bonded and unbonded prestressing tendons $(A_{psB} + A_{psU})f_{ps(WA)}$ (instead of $A_{psB}f_{psB} + A_{psU}f_{psU}$) to satisfy the moment equilibrium.




# ACI440 Design Guide and AASHTO Provisions

Accuracy of ACI 440.4R in predicting deflections and moment at cracking, yielding and ultimate carrying capacity.

| | $\Delta_{cr}$ | | $\Delta_y$ | | $\Delta_u$ | | $M_{cr}$ | | $M_y$ | | $M_u$ | | $\varepsilon_{cu}$ | |
|---|---|---|---|---|---|---|---|---|---|---|---|---|---|---|
| **Designation** | *ACI* | $\mu$ | *ACI* | $\mu$ | *ACI* | $\mu$ | *ACI* | $\mu$ | *ACI* | $\mu$ | *ACI* | $\mu$ | *ACI* | $\mu$ |
| **BS-2-3** | 2.03 | 0.31 | 9.91 | 0.76 | 21.08 | 0.15 | 2204 | 1.03 | 3346 | 1.08 | 4266 | 0.89 | 0.0024 | 0.77 |
| **BS-2-2** | 1.96 | 0.69 | 11.43 | 1.03 | 23.11 | 0.27 | 1690 | 1.21 | 2461 | 1.07 | 3956 | 1.12 | 0.0018 | 0.82 |
| **US-2-3** | 1.42 | 0.33 | 8.89 | 0.56 | 19.05 | 0.13 | 2009 | 1.05 | 3346 | 1.08 | 4399 | 0.92 | 0.0026 | 0.88 |
| **US-1-3** | 1.22 | 0.37 | 6.86 | 0.93 | 16.76 | 0.18 | 1151 | 0.88 | 1974 | 1.13 | 2549 | 0.90 | 0.0013 | 0.49 |
| **US-1-4** | 0.81 | 0.23 | 6.35 | 2.50 | 13.46 | 0.27 | 1522 | 1.36 | 2230 | 0.98 | 3487 | 1.09 | 0.0018 | 0.68 |
| **UF-1-3*** | 1.30 | 0.87 | 10.16 | 2.18 | 21.59 | 0.45 | 1336 | 0.99 | 2186 | 1.17 | 4107 | 1.05 | 0.0016 | 0.61 |
| **UF-1-3** | 1.55 | 0.62 | 12.19 | 0.76 | 26.16 | 0.45 | 1390 | 1.06 | 2230 | 1.37 | 2894 | 0.91 | 0.0018 | 0.63 |
| **UF-1-4** | 1.75 | 0.41 | 8.64 | 0.72 | 19.30 | 0.14 | 1708 | 1.26 | 2841 | 1.37 | 4027 | 0.99 | 0.0022 | 0.80 |
| **HS-U3-B3** | 1.65 | 0.31 | 7.37 | 0.68 | 17.27 | 0.13 | 2089 | 1.16 | 2956 | 1.18 | 4071 | 0.92 | 0.0022 | 0.74 |
| **HS-B3-U3** | 2.46 | 0.31 | 13.97 | 1.17 | 27.18 | 0.22 | 2115 | 1.00 | 3257 | 1.22 | 4620 | 1.08 | 0.0021 | 0.73 |
| **HS-B3-U4** | 2.62 | 0.54 | 11.18 | 0.70 | 23.62 | 0.22 | 2204 | 1.18 | 3089 | 0.82 | 5178 | 0.94 | 0.0029 | 1.03 |
| **HS-B4-U4** | 2.16 | 0.37 | 9.40 | 0.49 | 21.84 | 0.22 | 2815 | 1.22 | 2983 | 0.75 | 4992 | 0.85 | 0.0030 | 1.03 |
| **HF-B2-U3** | 2.01 | 0.67 | 10.41 | 0.65 | 22.35 | 0.33 | 2071 | 1.16 | 3841 | 1.14 | 3815 | 0.90 | 0.0022 | 0.98 |
| **HF-B2-U3d** | 2.51 | 0.66 | 16.00 | 0.93 | 30.48 | 0.40 | 2098 | 1.01 | 4098 | 1.17 | 4540 | 0.97 | 0.0024 | 1.24 |
| **HF-U3-B3** | 2.39 | 0.36 | 12.45 | 0.73 | 25.65 | 0.32 | 2664 | 1.08 | 3708 | 1.02 | 4779 | 0.90 | 0.0027 | 0.93 |
| **HF-B3-U3** | 1.37 | 0.33 | 6.60 | 0.29 | 15.49 | 0.16 | 2345 | 1.09 | 3346 | 1.02 | 4505 | 0.94 | 0.0025 | 0.86 |
| **HF-B3-U4** | 1.65 | 0.32 | 9.14 | 0.51 | 20.32 | 0.17 | 2478 | 1.05 | 4098 | 1.01 | 5125 | 0.88 | 0.0031 | 1.04 |
| **HF-B4-U3** | 1.78 | 0.59 | 11.18 | 2.21 | 23.88 | 0.30 | 2885 | 1.04 | 4204 | 0.87 | 5381 | 0.90 | 0.0029 | 0.92 |
| **Average mean Error (μ)** | | 0.46 | | 0.99 | | 0.25 | | 1.1 | | 1.08 | | 0.95 | | 0.84 |

- The average error for predicting the moment capacity at cracking, yielding and ultimate carrying capacity is found to be 1.1, 1.08, and 0.95, respectively, which is considered acceptable.
- The concrete compression strain was predicted with an average error around 0.84.
- ACI 440.4R underestimated cracking and ultimate deflections which has a direct effect on the ductility predictions of unbonded and hybrid beams.

# Finite Element Modeling

The trussed-beam analogy consists of four components: 1) Beam element (B21), 2) Truss element (T2D2), 3) Rigid Springs and 4) MPC connectors, are adopted and applied on the tested beams.

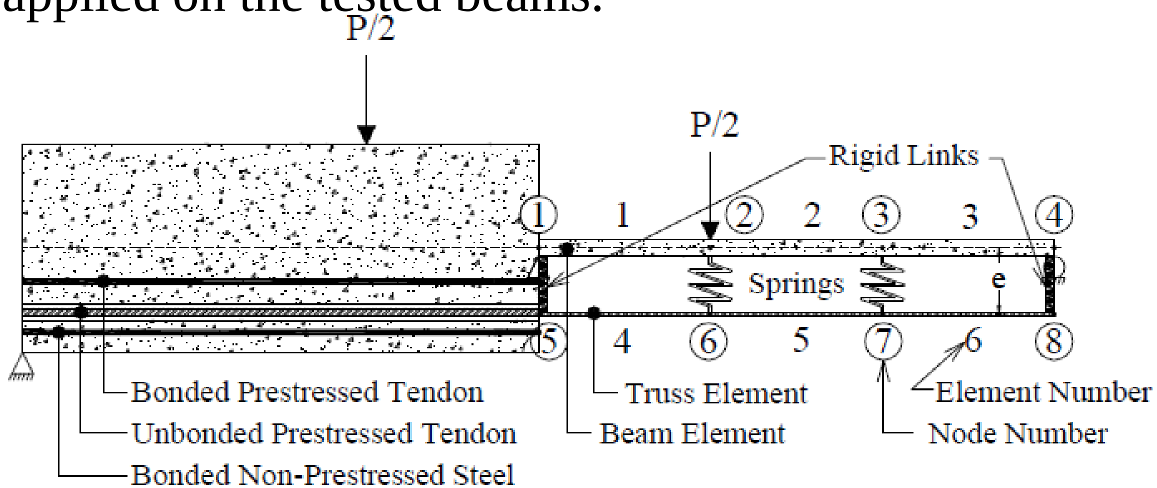


Idealized half-beam model (Nassif et al.2003)

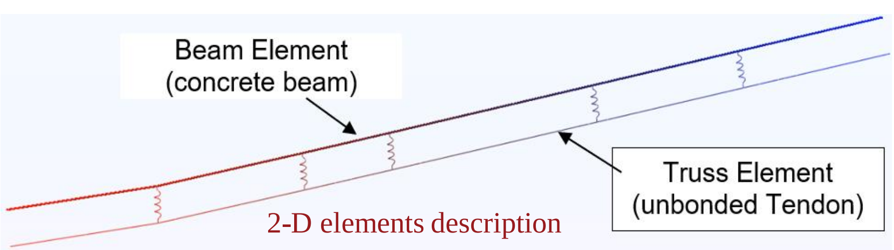


2-D elements description

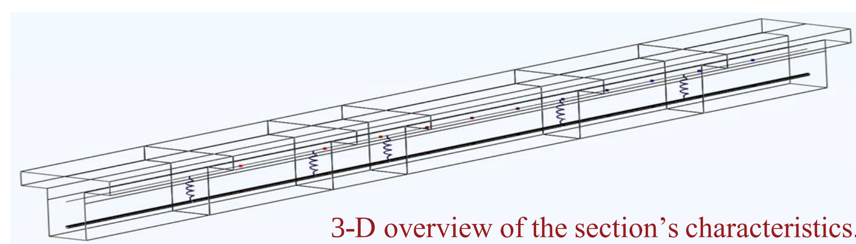

3-D overview of the section’s characteristics.

# Finite Element Modeling- Unbonded and Hybrid beams

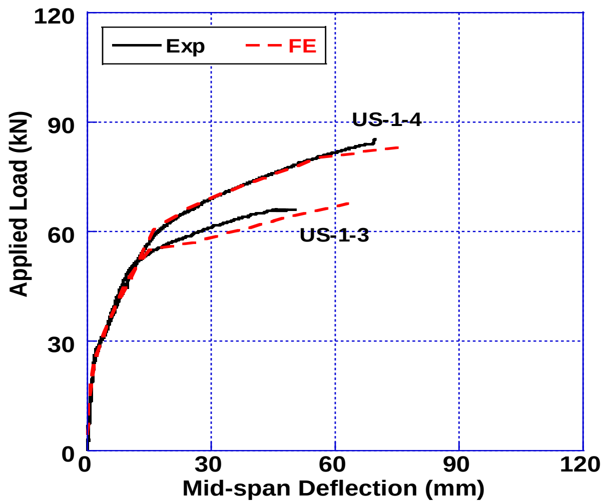


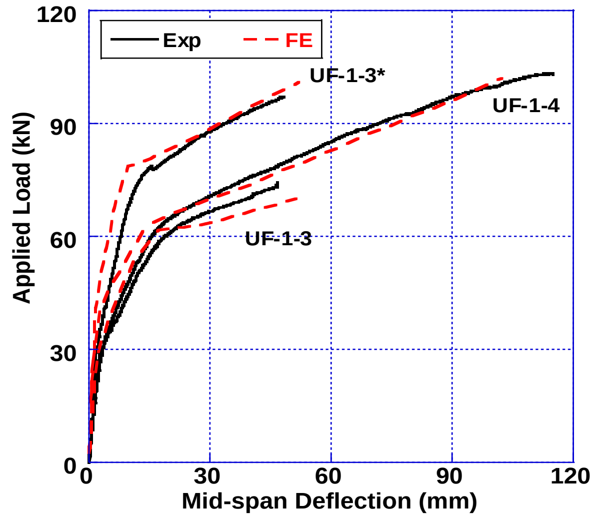


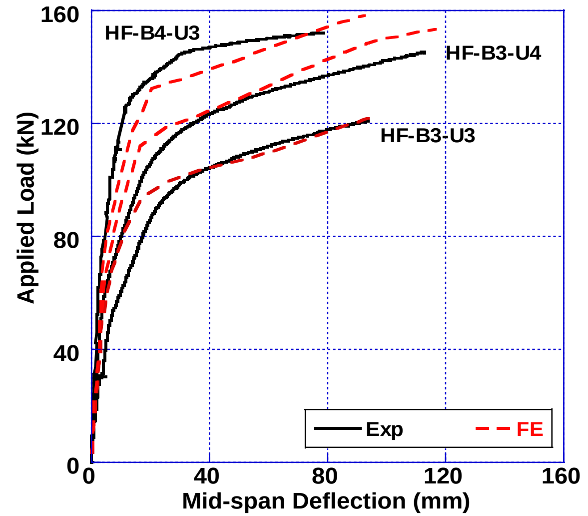


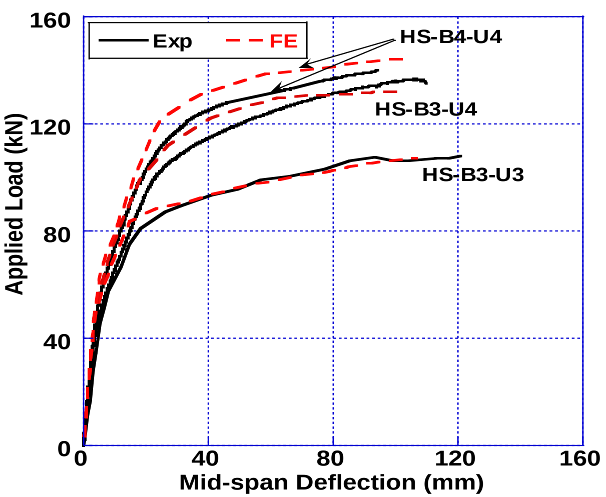


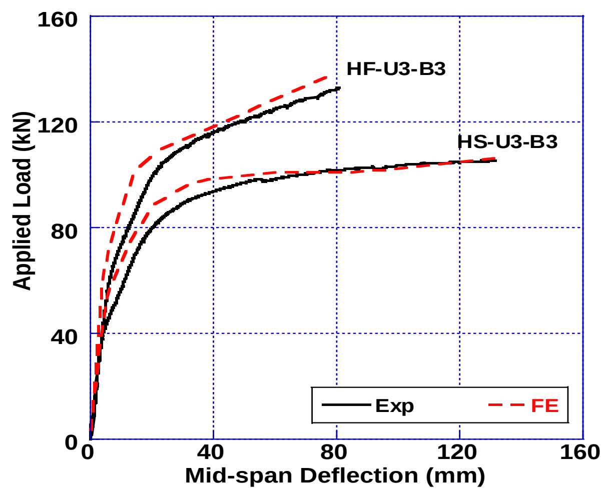

# Finite Element Modeling (cont’d)

| Designation | $P_{cr}$ | | | $P_u$ | | | $\Delta_{cr}$ | | | $\Delta_u$ | | |
|---|---|---|---|---|---|---|---|---|---|---|---|---|
| | Exp | FE | $\mu$ | Exp | FE | $\mu$ | Exp | FE | $\mu$ | Exp | FE | $\mu$ |
| US-1-3 | 33 | 32.5 | 0.99 | 71 | 74 | 1.04 | 3.3 | 3.2 | 0.97 | 92.7 | 83.6 | 0.90 |
| US-1-4 | 28 | 28.2 | 1.01 | 80 | 83 | 1.04 | 3.6 | 3.7 | 1.01 | 83.8 | 76.7 | 0.92 |
| UF-1-3* | 34 | 33.4 | 0.98 | 98 | 100 | 1.02 | 1.5 | 1.1 | 0.75 | 48.3 | 51.8 | 1.07 |
| UF-1-3 | 33 | 31.4 | 0.95 | 80 | 70 | 0.88 | 2.5 | 2.3 | 0.93 | 49.0 | 51.6 | 1.05 |
| UF-1-4 | 34 | 32.0 | 0.94 | 102 | 102 | 1.00 | 4.3 | 4.2 | 0.98 | 114.8 | 103.6 | 0.90 |
| HS-U3-B3 | 45 | 44.0 | 0.98 | 111 | 111 | 1.00 | 5.3 | 5.0 | 0.94 | 132.3 | 136.4 | 1.03 |
| HS-B3-U3 | 53 | 55.0 | 1.04 | 107 | 107 | 1.00 | 7.9 | 7.0 | 0.89 | 121.2 | 114.3 | 0.94 |
| HS-B3-U4 | 47 | 49.9 | 1.06 | 138 | 132 | 0.96 | 4.8 | 4.0 | 0.83 | 108.7 | 100.8 | 0.93 |
| HS-B4-U4 | 58 | 60.0 | 1.03 | 147 | 144 | 0.98 | 5.8 | 5.1 | 0.89 | 94.5 | 102.1 | 1.08 |
| HF-U3-B3 | 62 | 62.3 | 1.01 | 133 | 138 | 1.04 | 6.6 | 6.1 | 0.93 | 80.5 | 78.2 | 0.97 |
| HF-B3-U3 | 54 | 53.1 | 0.98 | 120 | 122 | 1.02 | 4.1 | 4.0 | 0.97 | 94.0 | 94.2 | 1.00 |
| HF-B4-U3 | 59 | 61.2 | 1.04 | 147 | 158 | 1.08 | 5.1 | 5.4 | 1.06 | 78.7 | 82.0 | 1.04 |

- The idealized truss-beam can be reliably used for a to predict deflection and loads for hybrid-CFRP beams at different stages of the loading.
- The model was able to predict the re cracking loads within an average mean error ($\mu$) of 1 with 0.97 mean error for the unbonded beams, 1.03 for the hybrid-steel and 1.01 for the CFRP-hybrid beams.
- Similarly, an average mean error was observed to 1 for the FE predictions for ultimate load, in which the average error was calculated to be 1, 1.03 and 1.01 for the unbonded beams, Hybrid-steel beams, and CFRP- hybrid beams respectively.
- For the deflection, FEM predicted the mid-span deflection observed at the first crack to be around 0.93 for all beams, in which hybrid-steel beams was predicted with an average error of 0.89 which is 10% lower than the average error calculated for hybrid -CFRP beams (0.99). For the ultimate deflections, the average error was 6% higher than the cracking deflection.

# Finite Element Modeling (cont'd)

ACI 440 predictions for the ductility of unbonded and hybrid beams is not well established in the code which results in relatively higher average error when predicting conventional or other ductility indices

| Designation | $M_{cr}$ | | $M_u$ | | $\mu_y$ | $\mu_{zou}$ |
|---|---|---|---|---|---|---|
| | ACI 440/Exp | FE/Exp | ACI 440/Exp | FE/Exp | ACI 440/Exp | ACI 440/Exp |
| US-1-3 | 0.88 | 0.99 | 0.90 | 1.04 | 0.51 | 2.44 |
| US-1-4 | 1.36 | 1.01 | 1.09 | 1.04 | 0.94 | 2.12 |
| UF-1-3* | 0.99 | 0.98 | 1.05 | 1.02 | 0.56 | 2.13 |
| UF-1-3 | 1.06 | 0.95 | 0.91 | 0.88 | 0.63 | 2.15 |
| UF-1-4 | 1.26 | 0.94 | 0.99 | 1.00 | 0.27 | 2.24 |
| HS-U3-B3 | 1.16 | 0.98 | 0.92 | 1.00 | 0.33 | 2.34 |
| HS-B3-U3 | 1.00 | 1.04 | 1.08 | 1.00 | 0.77 | 1.95 |
| HS-B3-U4 | 1.18 | 1.06 | 0.94 | 0.96 | 0.32 | 2.11 |
| HS-B4-U4 | 1.22 | 1.03 | 0.85 | 0.98 | 0.41 | 2.32 |
| HF-U3-B3 | 1.08 | 1.01 | 0.90 | 1.04 | 0.73 | 2.06 |
| HF-B3-U3 | 1.09 | 0.98 | 0.94 | 1.02 | 0.40 | 2.34 |
| HF-B4-U3 | 1.04 | 1.04 | 0.88 | 1.08 | 0.45 | 2.22 |
| ***Average μ*** | ***1.11*** | ***1.00*** | ***0.95*** | ***1.00*** | ***0.53*** | ***2.20*** |

## Conclusions

1) Hybrid steel-CFRP beams, utilizing CFRP as an unbonded element, is a robust prestressing system that can achieve extended service life due its inherent corrosion resistance, while maintaining a comparable serviceability performance compared with hybrid-steel beams.
2) Improvements in ductility and cracking load can be achieved with hybrid steel-CFRP prestressed beams when compared to hybrid-steel beams with effective reinforcement ratios equal or exceeding 0.06
3) ACI 440 predictions for the ductility of unbonded and hybrid beams needs to be revisited for consistency with conventional or other ductility indices. ACI 318 approach can be extended to hybrid beams.

# ACKNOWLEDGMENTS

The authors wish to express their gratitude and sincere appreciation for the support received in part from two Tier 1 University Transportation Centers (UTC):

1) RECAST at Missouri University of Science and Technology (MUST);
2) C2SMART: Connected Cities for Smart Mobility toward Accessible and Resilient Transportation at New York University,

and

3) New Jersey Department of Transportation (NJDOT) through the Bridge Resource Program (BRP) Project.

The contents of this presentation do not reflect the official views or policies of the supporting agencies.


# Questions?